Contents lists available at ScienceDirect

Applied Geochemistry

Origin and distribution of rare earth elements (REEs) in the soils of Meizhou City, southern China with high abundance of regolith-hosted REEs

Zhuoling Lin [a,b,e], Gaoling Wei [c], Jinlan Zhang [d], Xiaoliang Liang [a,e,f,*], Guangqing Huang [b,e,**]

[a] CAS Key Laboratory of Mineralogy and Metallogeny, Guangzhou Institute of Geochemistry, Chinese Academy of Sciences, Guangzhou, 510640, PR China
[b] Guangdong Public Laboratory of Geospatial Information Technology and Application, Guangzhou Institute of Geography, Guangdong Academy of Sciences, Guangzhou, 510070, PR China
[c] National-Regional Joint Engineering Research Center for Soil Pollution Control and Remediation in South China, Guangdong Key Laboratory of Integrated Agro-environmental Pollution Control and Management, Institute of Eco-environmental and Soil Sciences, Guangdong Academy of Sciences, Guangzhou, 510650, PR China
[d] Department of Information Engineering in Surveying Mapping and Remote Sensing, Guangdong Polytechnic of Industry and Commerce, Guangzhou, 510510, PR China
[e] University of Chinese Academy of Sciences, Beijing, 100049, PR China
[f] Guangdong Provincial Key Laboratory of Mineral Physics and Material Research & Development, Guangzhou, 510640, PR China

ARTICLE INFO

ABSTRACT

Currently, regolith-hosted rare earth element (REE) deposits in South China are the major source of global REEs, particularly heavy REEs (HREEs). This type of REE resource contains abundant movable, bioavailable, and ion-exchangeable REEs and may act as an environmental hazard; however, little is known regarding REEs in soils from areas with abundant deposits. Here, we investigated the REEs in the soil, surface water and crops, collected from Meizhou City, Guangdong Province, South China, as a representative region with abundant regolith-hosted REEs. Mean REE concentration (ΣREE) in the soil (318 μg g^{-1}) exceeded the local soil background (169 μg g^{-1}). The LREE/HREE ratio ranged from 2.04 to 69.4 in soil samples, suggesting the enrichment of light REEs (LREEs) compared with HREEs. Most soil samples exhibited positive Ce anomalies and negative Eu anomalies. The highest ΣREE (1162 μg g^{-1}) was detected in forest land, followed by garden land (793 μg g^{-1}) and paddy field (519 μg g^{-1}). According to the correlation analysis, pH as well as soil organic matter (SOM), Fe, and Mn content contributed to REE enrichment, while SOM and Mn content affected REE fractionation. REE enrichment in soil may be related to natural sources (e.g., parent materials) and anthropogenic activities (e.g., fertilizer application and coal combustion). The REE contamination of surface water was not serious. However, ΣREE in crops (7.08 μg g^{-1}·dw) indicated that these elements migrate from soils to plants, producing potential adverse effects on crops and humans. These findings shed new light on the geochemical behavior of REEs in the environments with abundant regolith-hosted REEs and can serve as a reference to prevent and control REE contamination.

1. Introduction

Rare earth elements (REEs) comprise lanthanides as well as Y and Sc, with an identical electron configuration, comprising six shells, large ionic radii, and (III) oxidation states (Prego et al., 2009). REEs are typically divided into two groups based on their atomic number and mass: light REEs (LREEs: La to Eu) and heavy REEs (HREEs: Gd to Lu) (Henderson, 1984).

Owing to their unique physical and chemical properties, REEs are widely applied in the renewable energy industry and high technology,

rendering them critical metals (Xu et al., 2017). Therefore, increasing attention has been devoted to the formation, exploration, and mining of REE deposits. Moreover, REE-based micronutrient fertilizers are widely used in agriculture because they improve crop quality and yield and enhance disease resistance (Boyko et al., 2011). However, above a certain threshold concentration, REEs can accumulate in animals and plants, ultimately entering the human body through the food chain. According to animal experiments, this leads to adverse effects on human health, such as severe damage to brain and reproductive system (Yu et al., 2020), lung and hepatocyte toxicity (Ma et al., 2011), and

---

cytotoxicity (Heller et al., 2019). Thus, REEs are considered as emerging contaminants, and their distribution in the environment, particularly in soils, has garnered great interest.

Factors contributing to REE enrichment in soils include natural processes and anthropogenic activities (Wang et al., 2022). Among these, the major natural process is soil formation, in which REEs primarily originate from the dissolution of REE-bearing minerals in the parent rocks. During the weathering, REEs leach from primary minerals and are either lost into the soil solution or immobilized by secondary minerals. These processes are affected by the variations in redox potential, pH, and adsorption/desorption reactions associated with soil organic matter (SOM), clay minerals and iron-manganese (hydr)oxides (Davranche et al., 2005). This further leads to fractionation across the REE group, which is a characteristic of Ce and Eu anomalies, as well as fractionation between LREEs and HREEs, owing to the slight variations in their physical and chemical properties, such as solubility, complexation ability, and redox activity. Anthropic activities include fertilizer application, mining, and industrial activities. For instance, in China, REEs have been used in agricultural production for over 40 years, substantially increasing REE levels in soil (Tyler, 2004). Additionally, it is noteworthy that China harbors approximately 40% of the global REE reserves and is responsible for over 85% of the global REE consumption (Dutta et al., 2016). Vast amounts of REEs are discharged into the environment through REE mining (Wang and Liang, 2015), tailing accumulation (Liu et al., 2019), and electronic equipment waste treatment (Tunsu et al., 2014). For instance, the Bayan Obo mine, the largest REE deposit ever found on the earth, has been mined for REEs for nearly 60 years. The total REE concentration in surface soil was found to be in the range of 150–18,891 µg g^{-1}, with an average value of 1906 µg g^{-1}. This value is significantly higher than the national average of China (197 µg g^{-1}) (Wei et al., 1991), but close to that of the Bayan Obo ores. Therefore, REE distribution in soils must be investigated, particularly in areas with abundant REEs.

In natural environments, REEs are primarily detected in phosphates, carbonates, silicates, and iron/manganese oxides (Ramos et al., 2016). However, in tropical and subtropical regions, typical ion-adsorption REE deposits are widespread, in which REEs do not exist as independent minerals but are adsorbed onto clays (60%–95% of the total REEs). The adsorbed REEs can be readily extracted through a simple leaching technique using ammonium sulfate solution via an ion-exchange process. This implies that most REEs are unstable and can easily contaminate the surrounding environment. Previous studies have investigated REE pollution in soils surrounding deposits under mining (Liu et al., 2022; Zhuang et al., 2017). In Ganzhou City, in the Jiangxi Province of South China, where the majority of these deposits are located, high REE levels have been detected found in tailing soils, with an average value of 392 µg g^{-1} (Liu et al., 2019), suggesting the underlying hazardous effects on residents through the ingestion of contaminated food. Compared to that in areas with exploited deposits, REE distribution in areas with unexploited deposits but abundant REEs has seldom been examined, but it should not be ignored. Meanwhile, compared to areas with exploited deposits, areas with unexploited deposits often have high population density and extensive farming activities. Moreover, under warm, humid climates and acid rains, the immobilized REEs can be easily mobilized and can migrate from regolith into the surrounding ecosystem (Liu et al., 2019; Wang et al., 2022), implying a severe environmental risk in areas with abundant regolith-hosted REEs.

Here, Wuhua County of the Meizhou City in the Guangdong Province of South China was selected as the study area. To date, numerous ion-adsorption REE deposits have been discovered in this area without mining, suggesting high REE abundance. Moreover, the soil and water environment quality of the Wuhua County is of great significance, since it is the major drinking water source and agricultural producer of the Guangdong–Hong Kong–Macao Greater Bay Area. Through the collection and analysis of samples collected from topsoil, surface water, and crops, the objectives of the present study were to (i) reveal the

distribution characteristics of REEs; (ii) compare the abundance of REEs in different types of lands; and (iii) assess the fate and potential risk of REEs.

2. Materials and methods

2.1. Sampling sites

The sampling sites were located in Huayang, Meilin and Longcun Towns, at 23°55′N to 24°12′N latitude and 115°18′E to 116°02′E longitude, within Wuhua County, Meizhou City, Guandong Province, South China (Fig. 1). Wuhua County has three mountains in the southwest and east, and the terrain gradually slopes from the southwest to northeast. Genetic types include structural erosion, structural denudation, karst accumulation, and erosion accumulation (Guan et al., 2019; Wang et al., 2020; Yang et al., 2019). The lithology is mainly granite porphyry, with small amounts of granodiorite and monzonite porphyry. The study area has a humid monsoon climate in the southern subtropical zone. The mean annual temperature is 21.2 °C, and the mean annual precipitation is ~1520 mm. The Qinjiang River flows through the sampling area. High temperature and rains facilitate the formation of red soil on the parent granite through weathering. Several ion-adsorption REE deposits have been discovered around the sampling area, such as Futang and Changtanggang.

2.2. Sampling method

The sampling area was approximately 614 km, with a 1 km × 1 km sampling network. A total of 180 soil samples were collected, including respectively 27, 34, and 119 samples from garden land, paddy field, and forest land. The samples were collected from the surface horizon (0–20 cm) using a bamboo shovel. The altitude of the sampling sites ranged from 110 to 960 m. Sites far from urban and industrial areas were selected to avoid the effect of social and industrial activities. After collection, the samples were immediately stored in polythene plastic bags for subsequent analysis. Before analysis in the laboratory, the samples were naturally air-dried, and plant roots, gravel, and other sundries were removed. Thereafter, the samples were divided using the quarter method, ground, and screened through 1.7 and 0.075 mm sieves.
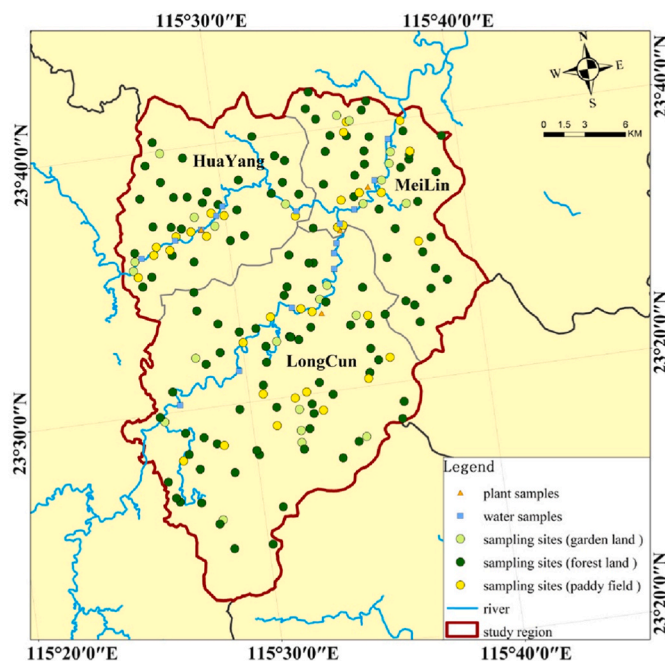

Fig. 1. Map of the sampling sites in the study area.

Sixteen water samples were collected from streams in the study area. These streams are less than 5 m wide and 30 cm deep. The obtained water samples were passed through a 0.45 μm PTFE filter for water chemistry analyses. To analyze of cation concentration, the samples were acidified to a pH of 2, and stored in 500 mL Teflon bottles. To analyze anion concentration, the samples were stored in 20 mL Teflon tubes without acidification. To measure total organic carbon (TOC) content, the samples were stored in 30 mL brown glass bottles, and mixed with 3 mL of H_2SO_4.

Eight crop samples were collected from the garden land: leaf mustard, sweet potato leaves, lettuce, shallot, cabbage, Chinese broccoli, *Brassica chinensis*, and peanut. After cleaning and drying, the edible parts of the crop samples were treated in an oven at 105 °C for 30 min, dried at 80 °C to a constant weight, and analyzed after crushing.

2.3. Analytical methods and quality control

The soil samples (0.1 g) were digested in a mixture of high-purity HNO_3 (6 mL) and HF (1 mL) in a microwave oven at 180 °C for 40 h. The samples were then dried at 180 °C, dissolved using $HClO_4$ (1 mL) until no residue was left, and further diluted with $HClO_4$ and HNO_3 for REE measurement. REE concentration was determined using inductively coupled plasma-mass spectrometry (ICP-MS, Agilent 7700x, USA), following a previously described procedure (Wang et al., 2018). Procedural blanks, replicate samples, and Chinese soil certified reference standards [GBW07447 (GSS-18) and GBW07387 (GSS-31)] were used in the batch analysis to monitor analytical precision and accuracy. Rh was used as the internal standard and was added to each sample for quantification. No quantifiable amounts of REE were detected in any of the procedural blanks. The analytical accuracy for REE was acceptable, with 80%–120% recovery. The analytical precision for REE was below 3% relative standard deviation (RSD). Fe, Al, Mn, Ca, Mg, K, and Na concentrations were measured using an inductively coupled plasma-atomic emission spectrometry (ICP-AES: Optima 3300 DV, PerkinElmer, USA) after digesting the soil samples with HNO_3–$HClO_4$–HF. pH was measured by equilibrating 10.0 g of sample particles (20 mesh) with 25 mL of de-ionized water in a capped beaker for 8 h. The liquid was collected by filtration, and its pH was measured using the Mettler-Toledo FiveEasy Plus™ pH meter with >0.05 precision.

All the water samples were analyzed for water chemistry [e.g., pH, electrical conductance (EC), oxidation–reduction potential (ORP), dissolved oxygen (DO), and ion and TOC concentration]. Water chemistry was analyzed directly in the field using a portable multifunctional testing instrument (HQ40d, Hach Water Analytical Instruments, Shanghai). The accuracy of determination was ±0.01 V for ORP, ±0.01 μS cm^{-1} for EC, ±0.1 for pH and ±0.1 mg L^{-1} for DO. REE concentration in water samples was analyzed using an ICP-MS (Agilent 7700x). Cation and anion concentrations were analyzed using the Dinex ion chromatographs (DX-500 and AQ-1100, respectively). TOC content was determined using a Shimadzu TOC-LCPH analyzer.

The collected crop samples were digested with HNO_3–HF–HCl–$HClO_4$ and analyzed using ICP-MS (Agilent 7700X). The accuracy of determination was ensured with the blank experiment (relative error <5%), repeated experiment (each measurement was repeated three times, standard deviation < 10%), and standard addition recovery methods.

2.4. REE fractionation analysis

REE distribution patterns in the soil, surface water, and crops were normalized using the North American Shale Composite (NASC) (Gromet et al., 1984). Following NASC normalization, the fractionations of REEs, as represented by LREE/HREE; Ce and Eu anomalies; and $(La/Yb)_N$, $(La/Sm)_N$, and $(Gd/Yb)_N$, were calculated. Ce and Eu anomalies were calculated as $\delta Ce = Ce_N/(La_N \times Pr_N)^{0.5}$ and $\delta Eu = Eu_N/(Sm_N \times Gd_N)^{0.5}$, respectively. δEu and δCe values exceeding 1.0 indicate Eu and Ce enrichment. In contrast, δEu and δCe values below 1.0 indicate depletion patterns of Eu and Ce.

The correlations of chemical parameters with REE enrichment and fractionation were analyzed using Prism (version 8.0.2). All correlations and differences were considered significant at P < 0.05.

3. Results and discussion

3.1. Soil REEs

The REE contents (ΣREE) of the soil was in the range of 60.5–1162 μg g^{-1} with an average of 318 μg g^{-1}; of this, La, Ce, and Nd accounted for 89.3% on average (Fig. 2 and Table S1). The $\sum$REE (mean [range] = 333 [131–793] μg·g^{-1}) in garden land was higher than that in paddy field (294 [95.5–518] μg·g^{-1}), while the $\sum$REEs in forest land was the most variable (310.8 [60.5–1162] μg·g^{-1}) (Fig. 2 and Table S1). On average, the soil REE concentration significantly exceeded the local soil background (170 μg g^{-1}), Chinese soil background (164 μg g^{-1}) (Wei et al., 1991) and the global crust background (154 μg g^{-1}) (Wang et al., 1989). Therefore, in the study region, the high abundance of regolith-hosted REEs has led to REE enrichment of the surface soil.

In all samples, ΣHREE and ΣLREE were in the range of 58.1–1056 and 2.41–151 μg g^{-1}, with average values of 294 and 24.1 μg g^{-1}, respectively. Thus, the LREE/HREE ratio varied from 2.04 to 69.4, indicating the relative enrichment of LREEs over HREEs in the soils. These results are consistent with the findings of most previous studies on REE distribution in mine tailings and the surrounding soils of regolith-hosted REE deposits (Liu et al., 2019; Zhou et al., 2020). Meanwhile, among already recognized deposits, nearly 90% were LREE-enriched, with $\sum$LREE oxides accounting for over 50% of the total REE resources (Li et al., 2017). This is also true for Wuhua County, where most of the identified deposits were LREE-enriched (Li et al., 2017). Moreover, compared with LREEs, HREEs possess a greater ability to form stable complexes with various ligands, such as carbonate and humic substances (Johannesson and Zhou, 1999); thus, HREEs can be preferentially removed from the upper horizons, resulting in the enrichment of LREEs in the top soil (Temga et al., 2021).

Contrary to other REEs that are stable in the trivalent state, Ce and Eu can form Ce^{4+} and Eu^{2+} under oxidative and reduced conditions, respectively, leading to Ce (δCe) and Eu (δEu) anomalies (Li et al., 2013; Mihajlovic et al., 2019). The δCe value ranged from 0.25 to 8.13, with an average of 1.50. Over 70% of the soil samples displayed positive Ce anomalies. In contrast, all the samples showed a significant and negative Eu anomalies, with the δEu value ranging from 0.12 to 1.32, with an average of 0.64. According to previous studies, the positive Ce and negative Eu anomalies are commonly observed in the topsoil. Eu can be easily reduced from Eu^{3+} to Eu^{2+}, and can migrate downward, generating a negative Eu anomaly (Chang et al., 2016). Meanwhile, Ce^{3+} in the soil solution can be easily oxidized to Ce^{4+} by atmospheric oxygen, which further co-precipitates to form $Ce(OH)_4$ and CeO_2. Secondary minerals are insoluble and enriched in the soil, resulting in the decoupling of Ce from other aqueous trivalent REE ions, leading to a positive Ce anomaly (Huang et al., 2021). Interestingly, three types of lands displayed the features of LREE enrichment, positive Ce anomaly, and negative Eu anomaly, but both the maximum and minimum of LREE/HREE ratios (69.4 and 2.04, respectively), δCe values (8.13 and 0.25, respectively), and δEu values (1.32 and 0.12, respectively) were recorded in the forest land. Therefore, the REE fractionation in forest land with less human activity is more inconstant than that in paddy field and garden land, even though they have developed on the homologous parent materials. This implies that, in addition to natural sources, REE distribution in these soils is also affected by anthropogenic activities (Mihajlovic et al., 2019).

In the study area, the mean $\sum$REE (318 μg g^{-1}) was close to the reported REE values in soil around ion-adsorption-type REE deposits and tailings (Huang et al., 2021; Liu et al., 2019), which highlights the high
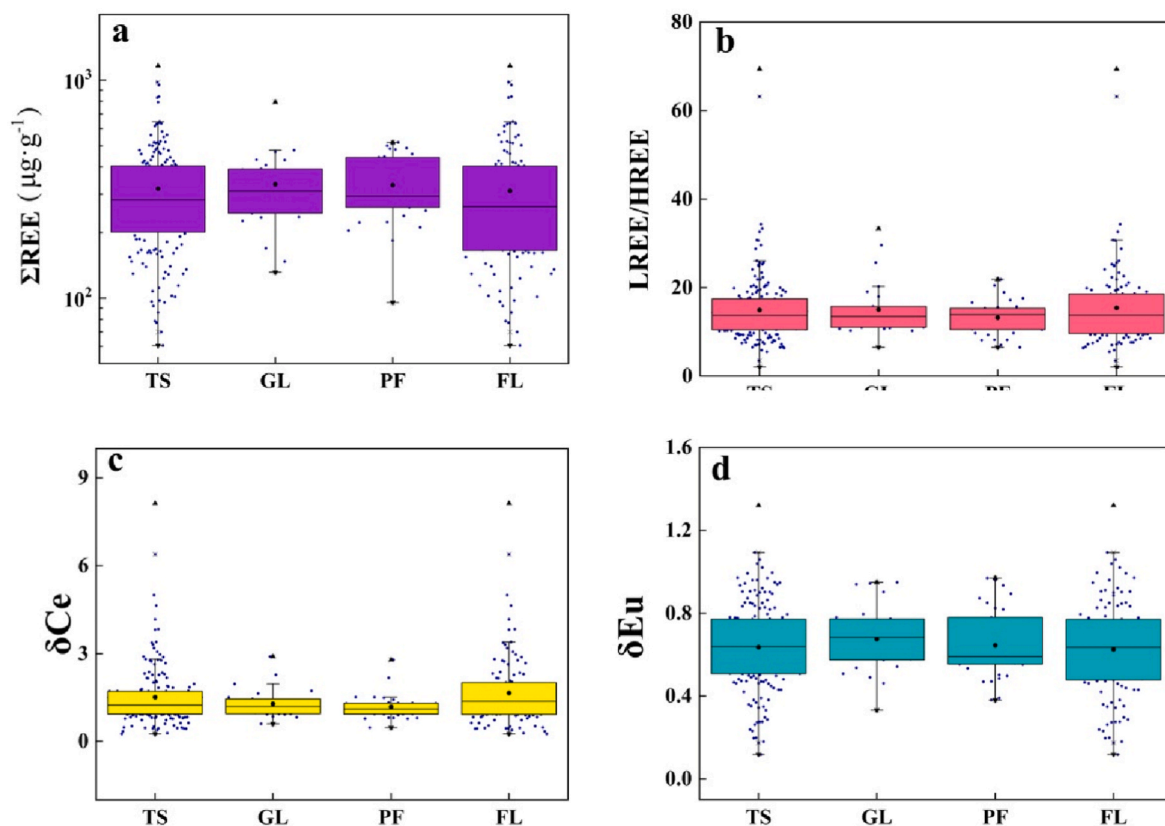
Fig. 2. Box diagrams distributions of ΣREE (a), LREE/HREE (b), δCe (c) and δEu (d) in soil samples from different land types. TS, GL, PF, and FL represent total soil samples, and those from garden land, paddy field, and forest land, respectively.

abundance of REEs in the region. Moreover, the average LREE/HREE ratio was 15.0, which is significantly higher than the local background value (7.8), suggesting the relative enrichment of LREEs. Of note, the highest ΣREE content (1163 µg g^{-1}) was recorded in forest land, followed by garden land (793 µg g^{-1}) and paddy field (519 µg g^{-1}). These values are higher than those of industrial-grade ion-exchangeable REE ores (500 µg g^{-1}) (Bao and Zhao, 2008). Since the study area is located in a subtropical region with abundant atmospheric precipitation, REE-bearing minerals are decomposed by acidic soil water at shallow levels in the weathering profile. Subsequently, REE^{3+} ions are prone to leaching into the leachate and migrating to the surrounding environments, such as soil, rivers, and groundwater. Compared with that of the main components (bedrock and weathering crust), the content of REEs in soil and water was lower, but it was sufficiently high and exceeded the standard value (Section 3.3). Thus, the physicochemical properties of soil and aquatic environments must be investigated to understand the transfer of REEs.

3.2. Soil physico-chemical properties

Soil pH in forest land ranged from 3.9 to 5.8, with an average of 4.7, which was slightly lower than that in garden land (4.7–7.2) and paddy field (4.6–6.1), with average values of 5.5 and 5.1, respectively (Table S2). This pH variation indicates an acidic soil environment in the study area. In contrast, SOM content in the forest land was in the range of 0.1–55.8 mg g^{-1} and an average of 13.8 mg g^{-1}, which was significantly lower than that in the garden land (9.6–39.5 mg g^{-1}) and paddy field (10.7–49.0 mg g^{-1}), with average values of 18.4 and 31.4 mg g^{-1}, respectively. Overall, the SOM content exhibited a decreasing trend in the order of paddy field > garden land > forest land. Compared with forest land, paddy field and garden land are greatly affected by fertilization and tillage, and these agricultural activities increase SOM

content. In terms of the content of major elements, the highest average values were recorded in garden land (42.4, 0.54, and 116 mg g^{-1} for Fe, Mn, and Al, respectively) (Fig. S1 and Table S2). Since the study area is dominated by laterite soil, intense weathering results in the enrichment of Fe and Al oxides in subtropical soil. Thus, the Fe and Al levels in all soils with different functions exceeded the Chinese national background value (29.4 and 66.2 mg g^{-1}, respectively).

Furthermore, the correlations of the above soil physicochemical properties with REE enrichment and fractionation characteristics were analyzed (Fig. 3). Herein, the (LREE/HREE)$_N$ ratio and total REE content, including the scenario in which LREEs and HREEs were considered separately, are considered the indicators of REE fractionation and enrichment, respectively. Low pH facilitates REE mobilization, while high pH induces REE precipitation (Wei et al., 2021). Thus, in forest land with less anthropogenic activity, pH was closely associated with ΣREE ($r = 0.256$, $p < 0.01$), ΣLREE ($r = 0.246$, $p < 0.01$), and ΣHREE ($r = 0.272$, $p < 0.01$). This trend is consistent with the previous findings that REEs in acidic soil environments are more likely to be activated during the weathering (Huang and Gong, 2001), promoting their migration into the surrounding environment. Interestingly, in both garden land and paddy field with intense agricultural activities, no significant correlation was noted between pH and ΣREE, ΣLREE, or ΣHREE.

In terms of the contents of major elements, both the Fe and Mn contents were significantly correlated with ΣREE (Fe: $r = 0.217$, $p < 0.05$; Mn: $r = 0.248$, $p < 0.01$), ΣLREE (Fe: $r = 0.212$, $p < 0.05$; Mn: $r = 0.231$, $p < 0.05$), and ΣHREE (Fe: $r = 0.206$, $p < 0.05$; Mn: $r = 0.322$, $p < 0.01$) in forest land. Owing to their large specific surface area, abundant surface hydroxyl groups, and high surface charges, Fe–Mn (hydr)oxides are considered important scavengers of REEs. Although the affinity of Fe (hydr)oxides and Mn (hydr)oxides for REEs differs, they typically coexist (Koeppenkastrop and De Carlo, 1992; Laveuf and Cornu, 2009; Liu et al., 2017; Pourret and Davranche, 2013), which
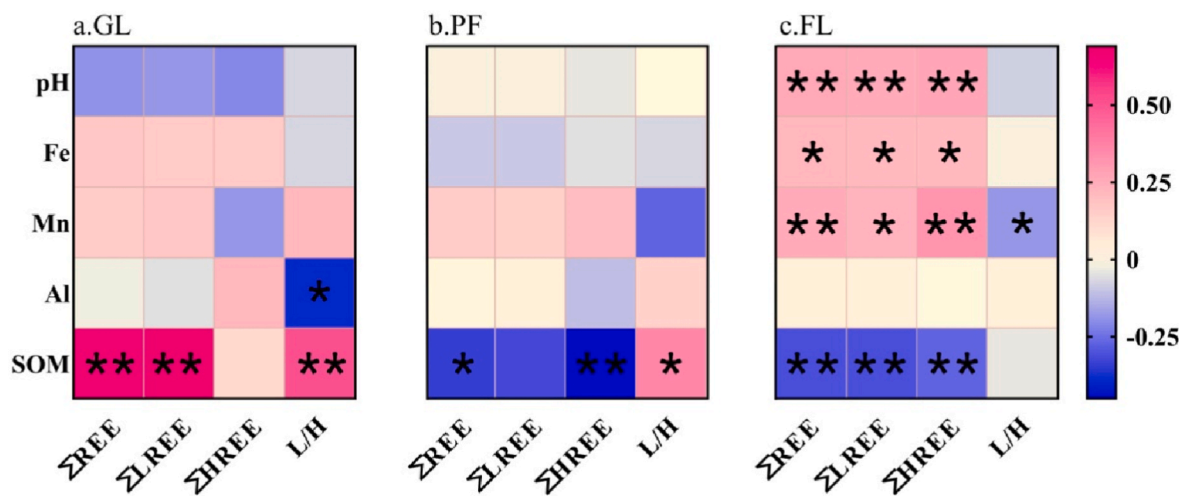
Fig. 3. Correlations of soil physicochemical properties (pH, SOM, Fe, Mn and Al) with REE enrichment and fractionation [e.g., ΣREE, ΣLREE, ΣHREE, and L/H (LREE/HREE)] in garden land (GL), paddy field (PF) and forest land (FL). *p < 0.05; **p < 0.01. Color bar scale represents correlation coefficients. r > 0, positive correlation; r < 0, negative correlation.

greatly contributes to REE enrichment. Moreover, Fe–Mn (hydr)oxides are important attenuators of heavy metals (Hockmann et al., 2014; Shi et al., 2020). In forest land, the Mn content exhibited a weak but significant negative correlation with LREE/HREE ($r = -0.181$, $p < 0.05$), suggesting the fractionation of REEs by Fe–Mn (hydr)oxides. As already noted in previous adsorption experiments, the surface hydroxyl groups of Fe–Mn (hydr)oxides can immobilize REEs through surface complexation, exhibiting a stronger adsorption capacity for HREEs. However, in garden land and paddy field, Fe and Mn contents were not closely correlated with ΣREE, ΣLREE, ΣHREE, and LREE/HREE, which is consistent with the lack of close correlation between pH and REE content in these land types. Thus, contrary to that in forest land, the enrichment and fractionation of REEs in garden land and paddy field may be affected by anthropogenic activities, including reclamation, planting, fertilization and irrigation, rather than natural processes (Liu et al., 2019). Previous studies have also provided another possible explanation that the effect of Fe–Mn (hydr)oxides on ΣREE varies with soil type and depth (Zhang and Shan, 2001). This may explain the lack of significant correlation between ΣREE and Fe and Mn contents in garden land and paddy field in the present study. In addition, no close correlation between Al content and ΣREE, ΣLREE, or ΣHREE was observed in any of the samples, as Al oxides, such as gibbsite, are not effective scavengers of REEs (Chang et al., 2016).

Functional groups can form complexes with REEs, and SOM can trap REEs. A previous study has revealed a positive correlation between SOM and REEs (Tang and Han, 2017). Interestingly, the correlation between REEs and SOM varied with land type in the present study. For instance, SOM showed a close positive correlation with ΣREE ($r = 0.673$, $p < 0.01$), and ΣLREE ($r = 0.692$, $p < 0.01$) in garden land (Fig. 3). However, significant negative correlations between SOM and ΣREE ($r = -0.313$, $p < 0.01$), ΣLREE ($r = -0.308$, $p < 0.01$) or ΣHREE ($r = -0.273$, $p < 0.01$) were observed in forest land. Additionally, there was a significant negative correlation between SOM and ΣREE ($r = -0.344$, $p < 0.05$) or ΣHREE ($r = -0.449$, $p < 0.01$) in paddy field. These trends may be attributed to the combined effects of natural processes (e.g., pH and redox conditions) and anthropogenic activities on REE enrichment (Davranche et al., 2011). In addition, SOM affects REE fractionation. LREE/HREE was significantly correlated with SOM in garden land ($r = 0.509$, $p < 0.01$), and paddy field ($r = 0.360$, $p < 0.05$) (Fig. 3). According to previous studies (Mihajlovic et al., 2019; Temga et al., 2021), HREEs can to more easily form complexes with bicarbonate than LREEs and can more readily migrate downward with eluviation. Meanwhile, LREEs tend to exist in the topsoil and are adsorbed by organic matter,

Fe–Mn (hydr)oxides, and clay minerals. With decrease in SOM content with soil depth, SOM content is positively correlated with LREE/HREE.

Based on our correlation analysis, the physico-chemical properties of soil greatly affect REE enrichment and fractionation. Specifically, soil pH and SOM, Fe, and Mn contents contribute to REE enrichment. Among these, SOM promotes REE enrichment in garden land soil, whereas pH and Fe and Mn contents show a significant impact in forest land. Overall, SOM and Mn content are vital factors for REE fractionation. In particular, SOM plays a pivotal role in garden land and paddy field, while Mn is of great importance in forest land and paddy field.

3.3. REE concentrations in surface water and plants

Although all the surface water samples were collected from the areas with similar geological backgrounds, the ΣREE values of most samples differed remarkably, fluctuating in the range of 0.048–2.41 μg L^{-1} (Table S3); REE content was undetected in several samples. The highest (2.41 μg L^{-1}) and average (0.643 μg L^{-1}) value were approximately nine and two higher than the background value of REE concentrations in Chinese water (0.27 μg L^{-1}) (Zhou et al., 2012). Previous studies have reported aqueous REE concentrations reaching as high as 13,046 μg L^{-1} around the REE mining areas in Jiangxi Province (Hao et al., 2016). In addition, REE contamination has been reported in several explored ion-adsorption REE deposits, with concentrations in rivers reaching 311 (Cao et al., 2019; Davranche et al., 2011), 553 (Olias et al., 2018), or 7730 μg L^{-1} (Liu et al., 2019), which are much higher than the value recorded in the present study. Therefore, as opposed to that in aquatic environments near deposits under mining, REE pollution was not detected in aquatic environments in areas with abundant regolith-hosted REEs but without mining activity.

Furthermore, the accumulation of REEs in plants, particularly crops, was analyzed, as they are important as food for humans and other organisms. The ΣREE of crops ranged from 1.74 to 11.8 μg g^{-1}·dw, with a mean of 7.08 μg g^{-1}·dw (Table S4), which was much higher than the national standard in China (0.7 μg g^{-1} fresh weight, GB2762-2005). Consistent with REE fractionation characteristics in garden land and paddy field, LREEs were relatively enriched, while HREEs were depleted in crops, suggesting nonselective absorption of HREEs and LREEs by crops. However, the studied crop species exhibited distinct REE accumulation ability. As such, the average ΣREE in leafy crops varied from 1.74 to 11.8 μg g^{-1}·dw, with an average of 6.98 μg g^{-1}·dw, while the value in root crop (i.e., peanut) was 7.79 μg g^{-1}·dw. The average ΣREE in crops decreased in the following order: leaf mustard > sweet potato

leaves > lettuce > peanut > cabbage > *Brassica chinensis* > Chinese broccoli > shallot (Table S4); thus, the ΣREE of crops depends on plant species, as well as REE mobility and bioavailability in soil (Loell et al., 2011). The detected contents were close to previously reported values for vegetables grown near the REE mining areas in Fujian (3.58 μg g^{-1}·dw) (Li et al., 2013), and Jiangxi (6.37 μg g^{-1}·dw) (Zhu et al., 2002) in China. In another recent study, an extremely high REE content (25.0 μg g^{-1}·dw) was reported in crops collected from an REE-abundant area in Guangzhou, China (Wang et al., 2022). Given the accumulation of REEs in plants and probability of their entry into the human body through the food chain, the risks of these contaminants to the residents of the study area cannot be ignored (Khan et al., 2017).

3.4. REE sources and transfer

To further identify the sources of REEs in the studied area, REE fractionation patterns were NASC-normalized to eliminate the "even––odd" effect. The obtained REE fractionation patterns in the soil samples were right oblique, with obvious LREE enrichment (average LREE/HREE = 12.2), a slight positive Ce anomaly, and Eu depletion (Fig. 4a and b). However, contrary to the REE fractionation in soils, the normalized fractionation patterns in the surface water exhibited remarkable LREE depletion and slight HREE enrichment (Fig. 4a), with

an average LREE/HREE of 0.796. This result may be attributed to the higher mobility of HREEs than that of LREEs due to their ability to form more stable complexes with inorganic ligands and organic ligands, leading to their preferential enrichment in surface water. However, as previously mentioned, the leaching of REEs from the soil into surface water does not cause apparent REE contamination.

In surface water, clay minerals and Fe–Al–Mn (hydr)oxides show strong adsorption properties toward REEs and act as pivotal REE carriers (Leybourne and Johannesson, 2008; Protano and Riccobono, 2002). Owing to the higher Fe–Al–Mn (hydr)oxides content in the surface water (Table S5), a lower content of free REE cations was detected. Based on Pearson correlation analysis (Table S6), REE content was not directly related to pH but was negatively correlated with Fe and Al content. Moreover, despite the significant correlation between Mn and ΣREE, low Mn content in the surface water suggests its negligible influence on REE enrichment.

The distribution patterns of REEs in crops were identical to those in soil, that is with LREE enrichment, stable HREE (average LREE/HREE = 13.2), and negative Eu anomalies (Fig. 4a). Therefore, REEs absorbed by crops inherited REE fractionation characteristics from soil. Nevertheless, the negative Ce anomaly in crops was more prominent than that in the soil, because Ce^{3+} can be easily oxidized to CeO$_2$ in the soil, which cannot be adsorbed by plants and preferentially stays in soils, as opposed
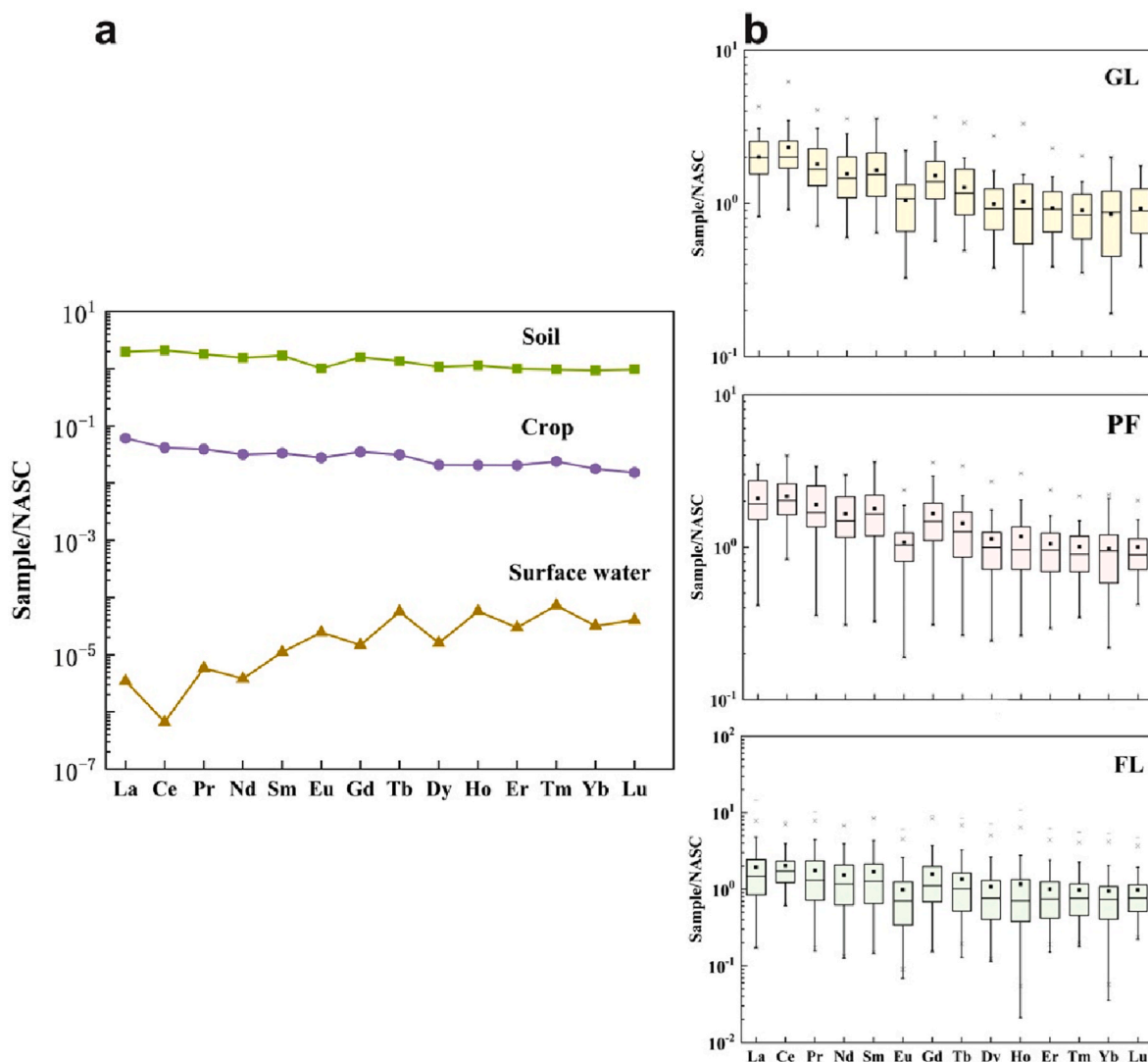

Fig. 4. NASC-normalized fractionation patterns of average REE values of 204 samples from soil (n = 180), surface water (n = 16) and crops (n = 8) (a), as well as from garden land (GL), paddy field (PF), and forest land (FL) (b).

to other REEs (Cao et al., 2001).

REE enrichment in soil is constrained by both pedogenesis and anthropogenic activity. The REE patterns of soils are mostly inherited from the parent rock. However, fertilizer addition to soils and other human activity also introduce exogenous REEs, which may lead to variations in the REE distribution characteristics (Wen et al., 2001). To discriminate the sources of REEs in the study area, REE fractionation feature in the soil was compared to that in the parent materials and some potential sources. The parent materials (local soil background) were selected as representative of the natural source, while chemical fertilization, vehicle exhaust, and coal combustion were selected as anthropogenic sources (Huang et al., 2019). Ternary plots of $(La/Yb)_N$ − $(La/Sm)_N$ − $(Gd/Yb)_N$ for the soil and potential sources were created (Fig. 5). The $(La/Yb)_N$, $(La/Sm)_N$, and $(Gd/Yb)_N$ values were in the range of 33.6%–54.3%, 10.7%–41.5%, and 19.5%–43.2% in garden land, 10.4%–37.6%, 15.3%–66.0%, and 14.8%–70.4% in paddy field, and 7.71%–61.9%, 10.2%–60.5% and 12.6%–47.3% in forest land, respectively. The distribution features of REEs in soils were close to those in the parent materials, chemical fertilization and coal combustion, but differed from those in vehicle emission (Fig. 5 and Text S1). This indicates that the REEs in soil might derived from parent materials, chemical fertilization and coal combustion. The sources of REEs in this study area are consistent with those in the paddy soils of Jiulong River Basin, Southeast China, which is also an area with high abundance of regolith-hosted REEs (Huang et al., 2019). Moreover, compared to the average $(La/Yb)_N$ and $(La/Sm)_N$ values of respectively 35.3% and 48.9% for the parent materials, 32.1% and 38.7% for coal combustion, and 30.6% and 26.1% for chemical fertilization, the average $(La/Yb)_N$ (>40%) was higher but the average $(La/Sm)_N$ (<26%) was lower for soil samples from garden and forest lands. Regarding $(Gd/Yb)_N$, the average for these soil samples (>33%) was slightly higher than for the parent materials (15.8%) and coal combustion (29.9%), but lower than that for chemical fertilization (43.3%). Conversely, for soil samples from paddy field, the average $(La/Yb)_N$, $(La/Sm)_N$ and $(Gd/Yb)_N$ was 21.1%, 33.7%, and 45.2%, respectively, which were more adjacent to those of chemical fertilization and coal combustion. Thus, compared to garden and forest lands, the REE distribution in paddy field were more affected by the anthropogenic activity, ascribed to the fact that paddy field receives more irrigation, planting and fertilization. This is in accord with the observation by previous study that REE fractionation in different land types was affected to various degrees by natural factors and anthropogenic activities (Zhou et al., 2020).

4. Conclusions

This present study investigated the distribution and origin of REEs in the soils of Meizhou City, Guangdong Province, Southern China with abundant regolith-hosted REE deposits. The average and highest of REE contents were 318 and 1163 mg kg^{-1}, respectively, with an obvious enrichment of LREEs relative to HREEs. Most soil samples exhibit positive Ce and negative Eu anomalies. The low pH and high Fe and Mn contents in the soil are conducive to the migration and enrichment of REEs in forest land soil, whereas the enrichment of REEs in paddy field and garden land soils can be ascribed to the synergistic effect of parent materials, chemical fertilization and coal combustion. The REE contamination of the surface water environment is not severe in the study area, but REE accumulation in crops is evident. Considering the frequent migration of these elements in the soil−water−crop systems, REEs in soils may negatively affect the public health through the food chain, which warrants attention.

Declaration of competing interest

The authors declare that they have no known competing financial interests or personal relationships that could have appeared to influence the work reported in this paper.
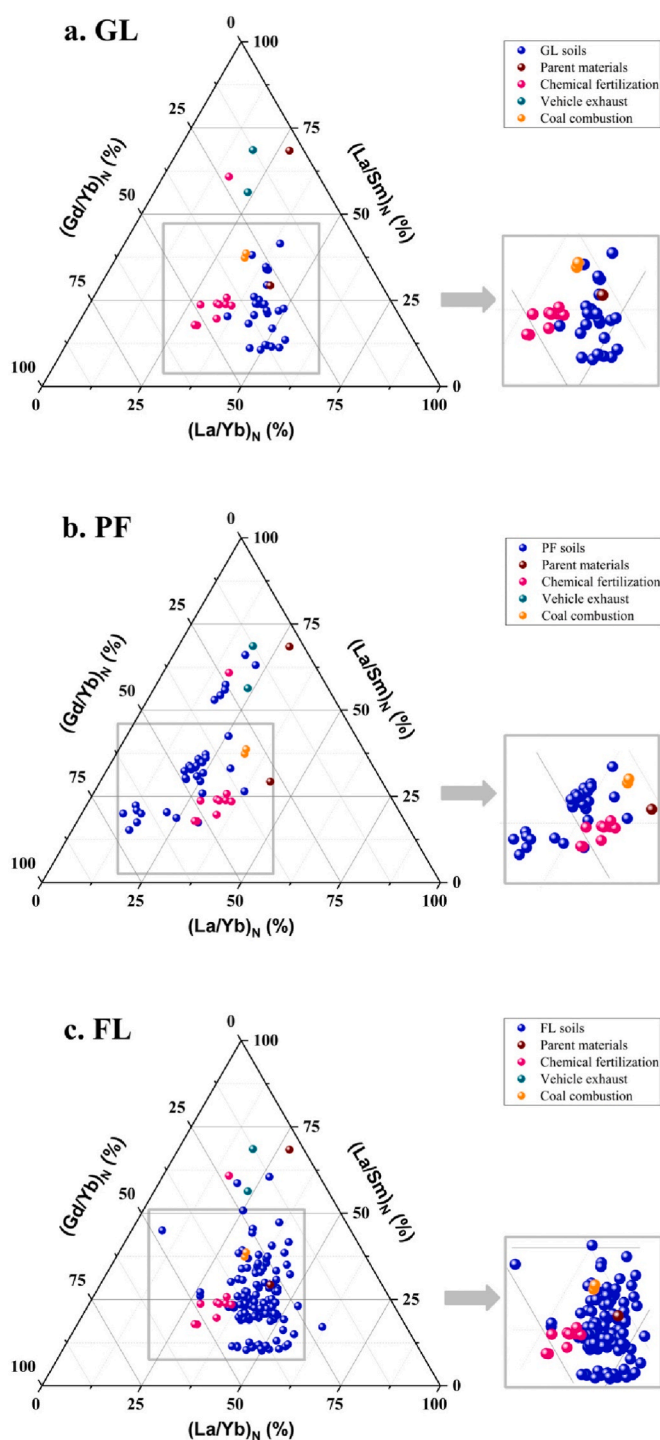

Fig. 5. Ternary plots of $(La/Yb)_N$ − $(La/Sm)_N$ − $(Gd/Yb)_N$ for REEs in garden land (a), paddy field (b), forest land (c) and several potential sources. The data of parent materials were sourced from background values of REEs in the soils of Guangdong Province (General Environment Monitor Station of China, 1990), and the data of chemical fertilization, coal combustion and vehicle emission were sourced from a previous study in the adjacent area (Huang et al., 2019).

Data availability

Data will be made available on request.

Appendix A. Supplementary data

Supplementary data to this article can be found online at https://doi.org/10.1016/j.apgeochem.2022.105514.

References

Bao, Z.W., Zhao, Z.H., 2008. Geochemistry of mineralization with exchangeable REY in the weathering crusts of granitic rocks in South China. Ore Geol. Rev. 33, 519–535.

Boyko, A., Matsuoka, A., Kovalchuk, I., 2011. Potassium chloride and rare earth elements improve plant growth and increase the frequency of the Agrobacterium tumefaciens-mediated plant transformation. Plant Cell Rep. 30, 505–518.

Cao, X.D., Chen, Y., Wang, X.R., Deng, X.H., 2001. Effects of redox potential and pH value on the release of rare earth elements from soil. Chemosphere 44, 655–661.

Cao, X.X., Zhou, S.Q., Xie, F., Rong, R., Wu, P., 2019. The distribution of rare earth elements and sources in Maoshitou reservoir affected by acid mine drainage, Southwest China. J. Geochem. Explor. 202, 92–99.

Chang, C.Y., Li, F.B., Liu, C.S., Gao, J.F., Tong, H., Chen, M.J., 2016. Fractionation characteristics of rare earth elements (REEs) linked with secondary Fe, Mn, and Al minerals in soils. Acta Geochemica. 35, 329–339.

Davranche, M., Pourret, O., Gruau, G., Dia, A., Le Coz-Bouhnik, M., 2005. Adsorption of REE(III)-humate complexes onto MnO_2: experimental evidence for cerium anomaly and lanthanide tetrad effect suppression. Geochem. Cosmochim. Acta 69, 4825–4835.

Davranche, M., Grybos, M., Gruau, G., Pédrot, M., Dia, A., Marsac, R., 2011. Rare earth element patterns: a tool for identifying trace metal sources during wetland soil reduction. Chem. Geol. 284, 127–137.

Dutta, T., Kim, K.H., Uchimiya, M., Kwon, E.E., Jeon, B.H., Deep, A., Yun, S.T., 2016. Global demand for rare earth resources and strategies for green mining. Environ. Res. 150, 182–190.

General Environment Monitor Station of China, 1990. Background Value of Chinese Soil Elements. Science Press, Beijing in Chinese.

Gromet, L.P., Dymek, R.F., Haskin, L.A., Korotev, R.L., 1984. The "North American shale composite": its compilation, major and trace element characteristics. Geochem. Cosmochim. Acta 48, 2469–2482.

Guan, L.J., Dong, H.W., Yang, Y.D., Bao, J.R., 2019. Geological Characteristics and Genesis of Rare Earth Deposits in Zhoujiang Area, Wuhua County, Guangdong Province. Xinjiang Nonferrous Metals, pp. 44–47 in Chinese.

Hao, X.Z., Wang, D.J., Wang, P.R., Wang, Y.X., Zhou, D.M., 2016. Evaluation of water quality in surface water and shallow groundwater: a case study of a rare earth mining area in southern Jiangxi Province, China. Environ. Monit. Assess. 188.

Heller, A., Barkleit, A., Bok, F., Wober, J., 2019. Effect of four lanthanides onto the viability of two mammalian kidney cell lines. Ecotoxicol. Environ. Saf. 173, 469–481.

Henderson, P., 1984. General geochemical properties and abundances of the rare earth elements. Dev. Geochem. 2, 1–32.

Hockmann, K., Tandy, S., Lenz, M., Schulin, R., 2014. Antimony leaching from contaminated soil under manganese- and iron-reducing conditions: column experiments. Environ. Chem. 11, 624–631.

Huang, C.M., Gong, Z.T., 2001. Geochemical implication of rare earth elements in process of soil development. J. Rare Earths 19, 57–62.

Huang, H.B., Lin, C.Q., Yu, R.L., Yan, Y., Hu, G.R., Wang, Q., 2019. Spatial distribution and source appointment of rare earth elements in paddy soils of Jiulong River Basin, Southeast China. J. Geochem. Explor. 200, 213–220.

Huang, J., Tan, W., Liang, X.L., He, H.P., Ma, L.Y., Bao, Z.W., Zhu, J.X., 2021. REE fractionation controlled by REE speciation during formation of the Renju regolith-hosted REE deposits in Guangdong Province, South China. Ore Geol. Rev. 134.

Johannesson, K.H., Zhou, X.P., 1999. Origin of middle rare earth element enrichments in acid waters of a Canadian High Arctic lake. Geochem. Cosmochim. Acta 63, 153–165.

Khan, A.M., Abu Bakar, N.K., Abu Bakar, A.F., Ashraf, M.A., 2017. Chemical speciation and bioavailability of rare earth elements (REEs) in the ecosystem: a review. Environ. Sci. Pollut. Res. 24, 22764–22789.

Koeppenkastrop, D., De Carlo, E.H., 1992. Sorption of rare-earth elements from seawater onto synthetic mineral particles: an experimental approach. Chem. Geol. 95, 251–263.

Laveuf, C., Cornu, S., 2009. A review on the potentiality of Rare Earth Elements to trace pedogenetic processes. Geoderma 154, 1–12.

Leybourne, M.I., Johannesson, K.H., 2008. Rare earth elements (REE) and yttrium in stream waters, stream sediments, and Fe–Mn oxyhydroxides: fractionation, speciation, and controls over REE + Y patterns in the surface environment. Geochim. Cosmochim. Acta 72, 5962–5983.

Li, X.F., Chen, Z.B., Chen, Z.Q., Zhang, Y.H., 2013. A human health risk assessment of rare earth elements in soil and vegetables from a mining area in Fujian Province, Southeast China. Chemosphere 93, 1240–1246.

Li, Y.H.M., Zhao, W.W., Zhou, M.F., 2017. Nature of parent rocks, mineralization styles and ore genesis of regolithhosted REE deposits in South China: an integrated genetic model. J. Asian Earth Sci. 148, 65–95.

Liu, H.Y., Pourret, O., Guo, H.M., Bonhoure, J., 2017. Rare earth elements sorption to iron oxyhydroxide: model development and application to groundwater. Appl. Geochem. 87, 158–166.

Liu, W.S., Guo, M.N., Liu, C., Yuan, M., Chen, X.T., Huot, H., Zhao, C.M., Tang, Y.T., Morel, J.L., Qiu, R.L., 2019. Water, sediment and agricultural soil contamination from an ion-adsorption rare earth mining area. Chemosphere 216, 75–83.

Liu, H.Y., Guo, H.M., Pourret, O., Wang, Z., Liu, M.H., Zhang, W.M., Li, Z.B., Gao, B., Sun, Z.X., Laine, P., 2022. Geochemical signatures of rare earth elements and yttrium exploited by acid solution mining around an ion-adsorption type deposit: role of source control and potential for recovery. Sci. Total Environ. 804.

Loell, M., Albrecht, C., Felix-Henningsen, P., 2011. Rare earth elements and relation between their potential bioavailability and soil properties, Nidda catchment (Central Germany). Plant Soil 349, 303–313.

Ma, J.Y., Zhao, H.W., Mercer, R.R., Barger, M., Rao, M., Meighan, T., Schwegler-Berry, D., Castranova, V., Ma, J.K., 2011. Cerium oxide nanoparticle-induced pulmonary inflammation and alveolar macrophage functional change in rats. Nanotoxicology 5, 312–325.

Mihajlovic, J., Bauriegel, A., Stark, H.J., Rosskopf, N., Zeitz, J., Milbert, G., Rinklebe, J., 2019. Rare earth elements in soil profiles of various ecosystems across Germany. Appl. Geochem. 102, 197–217.

Olias, M., Canovas, C.R., Basallote, M.D., Lozano, A., 2018. Geochemical behaviour of rare earth elements (REE) along a river reach receiving inputs of acid mine drainage. Chem. Geol. 493, 468–477.

Pourret, O., Davranche, M., 2013. Rare earth element sorption onto hydrous manganese oxide: a modeling study. J. Colloid Interface Sci. 395, 18–23.

Prego, R., Caetano, M., Vale, C., Marmolejo-Rodriguez, J., 2009. Rare earth elements in sediments of the vigo ria, NW iberian peninsula. Continent. Shelf Res. 29, 896–902.

Protano, G., Riccobono, F., 2002. High contents of rare earth elements (REEs) in stream waters of a Cu-Pb-Zn mining area. Environ. Pollut. 117, 499–514.

Ramos, S.J., Dinali, G.S., Oliveira, C., Martins, G.C., Moreira, C.G., Siqueira, J.O., Guilherme, L.R.G., 2016. Rare earth elements in the soil environment. Curr Pollut Rep 2, 28–50.

Shi, J.J., McGill, W.B., Chen, N., Rutherford, P.M., Whitcombe, T.W., Zhang, W., 2020. Formation and immobilization of Cr(VI) species in long-term tannery waste contaminated soils. Environ. Sci. Technol. 54, 7226–7235.

Tang, Y., Han, G.L., 2017. Characteristics of major elements and heavy metals in atmospheric dust in Beijing, China. J. Geochem. Explor. 176, 114–119.

Temga, J.P., Sababa, E., Mamdem, L.E., Bijeck, M.L.N., Azinwi, P.T., Tehna, N., Zame, P.Z., Onana, V.L., Nguetnkam, J.P., Bitom, L.D., Ndjigui, P.D., 2021. Rare earth elements in tropical soils, Cameroon soils (Central Africa). Geoderma Reg. 25.

Tunsu, C., Ekberg, C., Retegan, T., 2014. Characterization and leaching of real fluorescent lamp waste for the recovery of rare earth metals and mercury. Hydrometallurgy 144, 91–98.

Tyler, G., 2004. Rare earth elements in soil and plant systems - a review. Plant Soil 267, 191–206.

Wang, L.Q., Liang, T., 2015. Geochemical fractions of rare earth elements in soil around a mine tailing in Baotou, China. Sci. Rep. Uk 5.

Wang, Z., Yu, X., Zhao, Z., 1989. The Geochemistry of Rare Earth Elements. Science Press, Beijing in Chinese.

Wang, Z.B., Ma, J.L., Li, J., Wei, G.J., Zeng, T., Li, L., Zhang, L., Deng, W.F., Xie, L.H., Liu, Z.F., 2018. Fe (hydro) oxide controls Mo isotope fractionation during the weathering of granite. Geochem. Cosmochim. Acta 226, 1–17.

Wang, Z., Fu, S.C., Cao, H.J., Wang, C.H., Jiang, C.H., 2020. Comprehensive assessment of geological hazard risk: taking Wuhua county in Guangdong Province as an example. Miner. Explor. 11, 1470–1477.

Wang, Y., Wang, G., Sun, M., Liang, X., He, H., Zhu, J., Takahashi, Y., 2022. Environmental risk assessment of the potential "Chemical Time Bomb" of ion-adsorption type rare earth elements in urban areas. Sci. Total Environ. 822, 153305.

Wei, F., Liu, T., Teng, E., Rui, K., 1991. A survey on background contens of 15 rare earth elements in Chinese soil. Chin. J. Environ. Sci. 12, 78–82 in Chinese.

Wei, W., Ling, S.X., Wu, X.Y., Li, X.N., Liao, X., 2021. Investigations on mineralogy and geochemistry of a black shale profile on the northern Yangtze platform, China: weathering fate of rare earth elements and yttrium (REY) and its implications. Appl. Geochem. 126.

Wen, B., Yuan, D.A., Shan, X.Q., Li, F.L., Zhang, S.Z., 2001. The influence of rare earth element fertilizer application on the distribution and bioaccumulation of rare earth elements in plants under field conditions. Chem. Speciat. Bioavailab. 13, 39–48.

Xu, C., Kynicky, J., Smith, M.P., Kopriva, A., Brtnicky, M., Urubek, T., Yang, Y.H., Zhao, Z., He, C., Song, W.L., 2017. Origin of heavy rare earth mineralization in South China. Nat. Commun. 8.

Yang, M.J., Liang, X.L., Ma, L.Y., Huang, J., He, H.P., Zhu, J.X., 2019. Adsorption of REEs on kaolinite and halloysite: a link to the REE distribution on clays in the weathering crust of granite. Chem. Geol. 525, 210–217.

Yu, M., Yang, J.H., Gao, X., Sun, W.C., Liu, S.Y., Han, Y.R., Lu, X.B., Jin, C.H., Wu, S.W., Cai, Y., 2020. Lanthanum chloride impairs spatial learning and memory by inducing [Ca2+](m)overload, mitochondrial fission-fusion disorder and excessive mitophagy in hippocampal nerve cells of rats. Metallomics 12, 592–606.

Zhang, S.Z., Shan, X.Q., 2001. Speciation of rare earth elements in soil and accumulation by wheat with rare earth fertilizer application. Environ. Pollut. 112, 395–405.

Zhou, G.H., Sun, B.B., Liu, Z.Y., Wei, H.L., Zeng, D.M., Zhang, B.M., 2012. Geochemical feature of rare earthe lements in major rivers of Eastern China. Geoscience 26, 1028–1042.

Zhou, W.X., Han, G.L., Liu, M., Song, C., Li, X.Q., 2020. Geochemical distribution characteristics of rare earth elements in different soil profiles in mun River Basin, northeast Thailand. Sustain. Basel. 12.

Zhu, J.H., Yuan, Z.K., Wang, X.Y., Yan, S.M., 2002. Investigation on the contents of rare earth elements in environment of rare earth ore area in Jiangxi. J. Envrion Health 19, 443–444.

Zhuang, M.Q., Zhao, J.S., Li, S.Y., Liu, D.R., Wang, K.B., Xiao, P.R., Yu, L.L., Jiang, Y., Song, J., Zhou, J.Y., Wang, L.S., Chu, Z.H., 2017. Concentrations and health risk assessment of rare earth elements in vegetables from mining area in Shandong, China. Chemosphere 168, 578–582.